Errors in Detection of RF Pulses Embedded in Time Crosstalk, Frequency Crosstalk, and Noise

By E. A. MARCATILI

(Manuscript received September 21, 1960)

The probability of error in the detection of RF pulses embedded in a combination of Gaussian noise, time crosstalk from the tails of two neighboring pulses, and frequency crosstalk from an adjacent channel, is calculated.

It is shown that for a given probability of error it is possible to maximize the pulse repetition frequency and simultaneously to minimize the channel spacing and signal-to-thermal noise by operating the system at a signal-to-thermal noise level close to the level of the combined time and frequency crosstalk.

I. INTRODUCTION

Consider many PCM messages occupying adjacent frequency bands in the same transmission medium, as, for example, in the proposed long distance waveguide communication system.[1] At some point the messages must be separated and read; these operations are performed by the receivers. Each receiver will be considered to consist of a filter and an envelope detector that takes periodic instantaneous samples and decides if the level of the signal is above or below a threshold.

Suppose that at a certain sampling time there is no pulse to be detected. Nevertheless, the received signal will be composed of the summation of three types of interference: time crosstalk or intersymbol interference, frequency crosstalk, and noise.*

Time crosstalk is measured by the envelope of the message at the sampling time in the absence of other messages and noise; it is due to the trailing and leading edges of the other pulses that make the message. It is known that if the sampling is instantaneous the time crosstalk can be reduced to zero by proper choice of filters and input signal,[2] but in a

* Throughout this paper we understand "noise" to be thermal noise.

real system the sampling time is not zero, and consequently the intersymbol interference varies during that time. The actual description of how this varying crosstalk influences the detected signal is a very complicated problem that involves a detailed knowledge, not only of the input pulses and transfer characteristics of transmitters and receivers, but also of the detector. We by-pass this problem by assuming conservatively a fictitious system that indeed has instantaneous sampling, but with the time crosstalk being the maximum value achieved by the time crosstalk in the real system during the finite sampling time.

Frequency crosstalk is measured by the envelope at the sampling time in the absence of the wanted message and the noise; it is due to the fact that the other messages have spectrums that overlap with the transfer characteristic of the receiving filter of the channel under consideration.

Finally, noise is measured by the envelope at the sampling time in the absence of all the messages; it comes essentially from the first amplifier in the receiver.

If the envelope of the three interferences is bigger than the slicing level, the detector decides that a pulse exists in that time slot, and an error is made. Similarly, the detector makes another error if a pulse should be detected but is shadowed by the interferences in such a way that the envelope of the received signal is smaller than the slicing level.

It is the purpose of this paper first to determine the relationship between the amplitudes of the wanted signal, time crosstalk, frequency crosstalk, noise, and slicing level; and second to establish in some sense the most efficient design of a system for a given probability of error.

II. DENSITY DISTRIBUTION OF SIGNAL, TIME CROSSTALK, FREQUENCY CROSSTALK, AND GAUSSIAN NOISE

Simplifying assumptions:

(a) Time crosstalk is represented by the sum of two sine waves of the same amplitude and arbitrary phases. The implications are: First, only the trailing edge of the preceding pulse and the leading edge of the following one are important. Second, each received pulse is symmetrical. This is rigorously true if the input pulse is symmetrical and the system has no phase distortion. Third, the phases of the pulses are uncorrelated, which is true if the pulses have passed through several partially regenerative repeaters.

(b) Frequency crosstalk is represented by a sine wave of arbitrary phase. The implications are: First, only one neighboring channel feeds

non-negligible power into the wanted channel. This is shown to be a reasonable assumption in Appendix A. Second, the pulses in different channels are synchronized. If they were not, the amplitude of the frequency crosstalk would vary between the two extreme values that can be obtained with the best and the worst interleaving of pulses.

(c) The noise is assumed to be Gaussian.

(d) The detector measures instantaneously if the envelope of the received signal is above or below a threshold. This is probably the crudest approximation, because in a real system the detector is not ideal and, what is even worse, the signal passes through repeaters with only partial regeneration.

The vector representing the signal to be detected is

$$S = A + \rho_T e^{i\theta_1} + \rho_T e^{i\theta_2} + \rho_F e^{i\theta_3} + \text{Gaussian noise}, \tag{1}$$

where A is the amplitude of the RF of the wanted pulse; its value is one if there is a pulse to be detected, and zero if there is no pulse; its phase is taken as reference. The second and third term represent the time crosstalk; they are vectors of the same modulus ρ_T, but arbitrary phases θ_1 and θ_2. The fourth term represents the frequency crosstalk of modulus ρ_F and arbitrary phase θ_3. Each one of these three last vectors, being originated from binary pulses, has a 50-50 chance of being present or not. The bivariate density distribution,* calculated in Appendix B, (52) is

$$\begin{aligned} p(x,y) = \frac{e^{-r^2/2\sigma^2}}{16\pi\sigma^2}\Bigg[1 &+ 2e^{-\rho_T{}^2/2\sigma^2} I_0\left(\frac{\rho_T r}{\sigma^2}\right) + e^{-2\rho_T{}^2/\sigma^2} I_0{}^2\left(\frac{\rho_T r}{\sigma^2}\right) \\ &+ e^{-\rho_F{}^2/2\sigma^2} I_0\left(\frac{\rho_F r}{\sigma^2}\right) + 2e^{-(\rho_T+\rho_F)^2/2\sigma^2} I_0\left(\frac{\rho_T r}{\sigma^2}\right) I_0\left(\frac{\rho_F r}{\sigma^2}\right) \\ &+ e^{-(2\rho_T+\rho_F)^2/2\sigma^2} I_0{}^2\left(\frac{\rho_T r}{\sigma^2}\right) I_0\left(\frac{\rho_F r}{\sigma^2}\right)\Bigg], \end{aligned} \tag{2}$$

where x and y are the coordinates of the terminus of S, the vector representing the signal to be detected; $r = \sqrt{(x-A)^2 + y^2}$; σ^2 is the mean noise power; and I_0 is the modified Bessel function of first kind of order zero. The density distribution (2) is only valid for the tail of the distribution; that is,

$$\left.\begin{matrix}\rho_T \\ \rho_F\end{matrix}\right\} \ll r. \tag{3}$$

* For tutorial background see, for example, Bennett.[3]

It is possible to interpret the meaning of each term in (2). The first one is the contribution to $p(x,y)$ when only noise is present; on the average, this combination happens once each eight detections. The second term is the contribution when noise and only one of the two time crosstalk tails are present; on the average, this combination occurs once each four detections. The third term is the contribution when noise and both time crosstalk tails are present; on the average, this combination occurs once each eight detections. The fourth term is the contribution when noise and frequency crosstalk are present; on the average, this combination occurs once each eight detections. The fifth term is the contribution when noise, frequency crosstalk, and one time crosstalk tail are present; on the average, this combination occurs once each four detections. The sixth term is the contribution when noise, the two time crosstalk, and frequency crosstalk are present; on the average, this combination happens once each eight detections.

If there is a pulse to be detected (pulse on), A is equal to one and the density distribution (2) is

$$p(x,y) = p_1(x,y) \qquad (A = 1). \tag{4}$$

If there is no pulse to be detected (pulse off), A is zero and the density distribution is

$$p(x,y) = p_2(x,y) \qquad (A = 0). \tag{5}$$

Both functions, $p_1(x,y)$ and $p_2(x,y)$, schematically plotted as Figs. 1(a) and 1(b), have the same bell shape and circular symmetry around their respective axes located at $x = 1$, $y = 0$, and at $x = y = 0$.

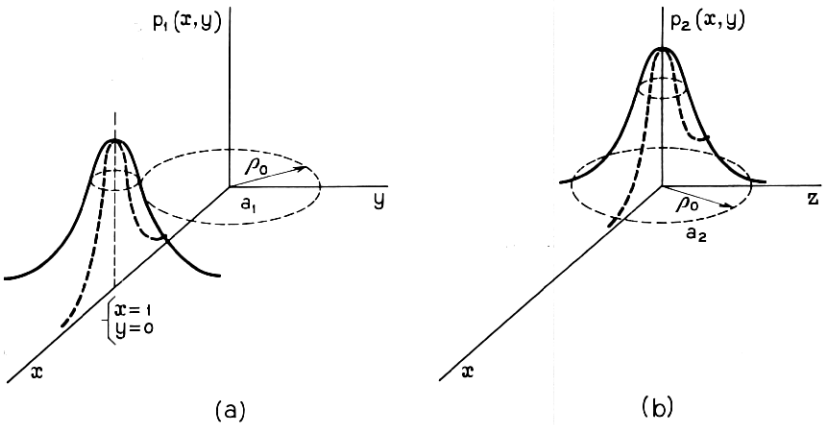

Fig. 1 — Density distribution for (a) pulse on, (b) pulse off.

III. PROBABILITY OF ERROR

In general, the volume defined by

$$P = \int_a p(x,y)\, dx\, dy \tag{6}$$

measures the probability that the signal S be a vector originating at the origin of coordinates and terminating at any point within the area of integration a.

The quantity $(1 - P)$ measures the probability that S is a vector with the terminus outside the area a. The detector decides whether the terminus is inside or outside of a.

Suppose that the signal free of interference A has its terminus outside of the area a; then if the received signal S is also outside of a the detector makes a correct decision, but if S falls inside of a the detector makes an error. Since the probability of finding S inside of a is given by P, this integral measures the probability of error and $(1 - P)$ measures the probability of making a correct decision.

The detector we use is one capable of deciding if the envelope of the received signal is bigger or smaller than a threshold ρ_0.

The probability of error in the "on pulse" condition, Fig. 1(a), is the probability that $|S| < \rho_0$:

$$P_1 = \int_{a_1} p_1(x,y)\, dx\, dy, \tag{7}$$

where $p_1(x,y)$ is derived from (2) by setting $A = 1$, and a_1 is the circle of radius ρ_0 and center at the origin of coordinates. The integration performed in Appendix C yields (70):

$$\begin{aligned} P_1 = \frac{K_0\left[\frac{(1-\rho_0)^2}{2\sigma^2}\right]}{16\pi}\Bigg[1 &+ 2e^{-\rho_T^2/2\sigma^2} I_0\left(\rho_T \frac{1-\rho_0}{\sigma^2}\right) \\ &+ e^{-2\rho_T^2/\sigma^2} I_0^2\left(\rho_T \frac{1-\rho_0}{\sigma^2}\right) + e^{-\rho_F^2/2\sigma^2} I_0\left(\rho_F \frac{1-\rho_0}{\sigma^2}\right) \\ &+ 2e^{-(\rho_T+\rho_F)^2/2\sigma^2} I_0\left(\rho_T \frac{1-\rho_0}{\sigma^2}\right) I_0\left(\rho_F \frac{1-\rho_0}{\sigma^2}\right) \\ &+ e^{-(2\rho_T+\rho_F)^2/2\sigma^2} I_0^2\left(\rho_T \frac{1-\rho_0}{\sigma^2}\right) I_0\left(\rho_F \frac{1-\rho_0}{\sigma^2}\right)\Bigg], \end{aligned} \tag{8}$$

where I_0 is the modified Bessel function of the first kind of order zero and K_0 is the modified Bessel function of the second kind of order zero.

The probability of error in the "off pulse" condition, Fig. 1(b), is the probability that $| S | > \rho_0$:

$$P_2 = \int_{a_2} p_2(x,y)\, dx\, dy, \tag{9}$$

where $p_2(x,y)$ is obtained from (2) by making $A = 0$, and a_2 is the surface outside a_1. The integration performed in Appendix C yields (77):

$$\begin{aligned} P_2 = \frac{e^{-\rho_0^2/2\sigma^2}}{8}\Bigg[1 &+ 2e^{-\rho_T^2/2\sigma^2} I_0\left(\frac{\rho_T\rho_0}{\sigma^2}\right) + e^{-2\rho_T^2/\sigma^2} I_0^2\left(\frac{\rho_T\rho_0}{\sigma^2}\right) \\ &+ e^{-\rho_F^2/2\sigma^2} I_0\left(\frac{\rho_F\rho_0}{\sigma^2}\right) + 2e^{-(\rho_T+\rho_F)^2/2\sigma^2} I_0\left(\frac{\rho_T\rho_0}{\sigma^2}\right) I_0\left(\frac{\rho_F\rho_0}{\sigma^2}\right) \\ &+ e^{-(2\rho_T+\rho_F)^2/2\sigma^2} I_0^2\left(\frac{\rho_T\rho_0}{\sigma^2}\right) I_0\left(\frac{\rho_F\rho_0}{\sigma^2}\right)\Bigg], \end{aligned} \tag{10}$$

with I_0 and K_0 being the modified Bessel functions of the first and second kinds.

The six terms appearing in expressions (8) and (10) have the same physical interpretation as that given for the six terms appearing in (2).

Since the "on" and "off" pulses are equally likely, the probability of error of the message is

$$P = \tfrac{1}{2}(P_1 + P_2). \tag{11}$$

The probability of error of the message P can be calculated for any combination of time and frequency crosstalk ρ_T and ρ_F, but it is possible to relate these two values by demanding that, according to some rule, both are equally damaging to the system. The rule we adopt is given by the following equations:

$$\begin{aligned} P_1(\rho_F = 0, \quad \rho_0 = 0.5) &= P_1(\rho_T = 0, \quad \rho_0 = 0.5); \\ P_2(\rho_F = 0, \quad \rho_0 = 0.5) &= P_2(\rho_T = 0, \quad \rho_0 = 0.5). \end{aligned} \tag{12}$$

For any signal-to-noise level and a slicing level equal to half the pulse amplitude ($\rho_0 = 0.5$), the probability of error in the "on" or "off" pulse condition due to noise and only time crosstalk is equal to that due to noise and only frequency crosstalk.

Substituting (8) and (10) in equation (12), we get

$$2e^{-\rho_T^2/2\sigma^2} I_0\left(\frac{\rho_T}{2\sigma^2}\right) + e^{-2\rho_T^2/\sigma^2} I_0^2\left(\frac{\rho_T}{2\sigma^2}\right) - 1 = 2e^{-\rho_F^2/2\sigma^2} I_0\left(\frac{\rho_F}{2\sigma^2}\right). \tag{13}$$

Frequency crosstalk ρ_F has been plotted against time crosstalk ρ_T, for different signal-to-noise levels $1/\sqrt{2}\sigma$ in Fig. 2.

A line defined by the following equation

$$20 \log \frac{1}{\rho_T} = 20 \log \frac{1}{\rho_F} + 3$$

has been included in the same figure (dotted line) for comparison purposes. Either from (13) or from Fig. 2 it can be deduced that for

$$\frac{\rho_T}{2\sigma^2} \ll 1, \qquad \rho_F \cong \sqrt{2}\rho_T \tag{14}$$

and for

$$\frac{\rho_T}{2\sigma^2} \gg 1, \qquad \rho_F \cong 2\rho_T. \tag{15}$$

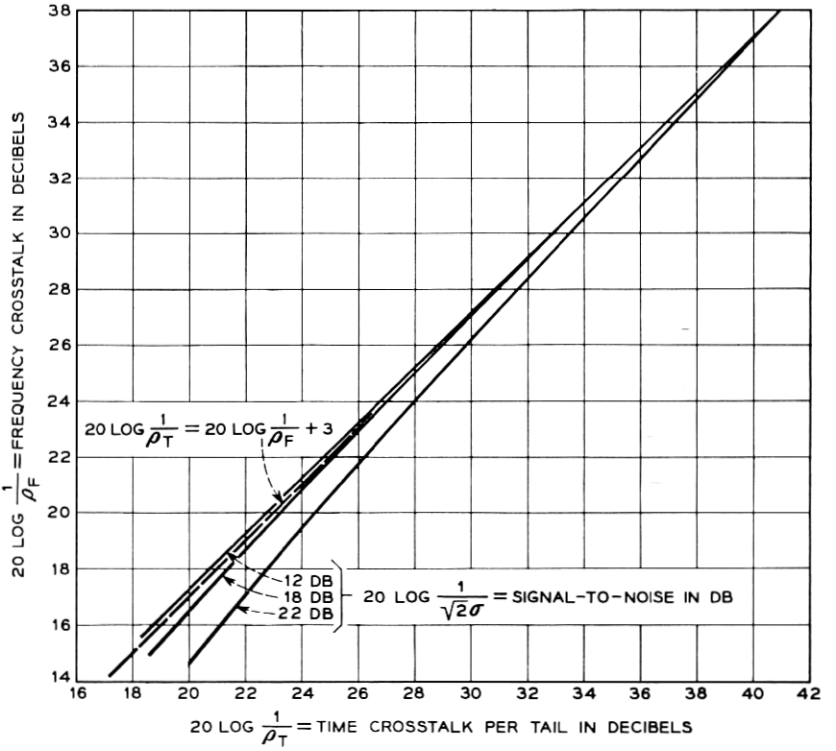

Fig. 2 — Equally damaging time and frequency crosstalk.

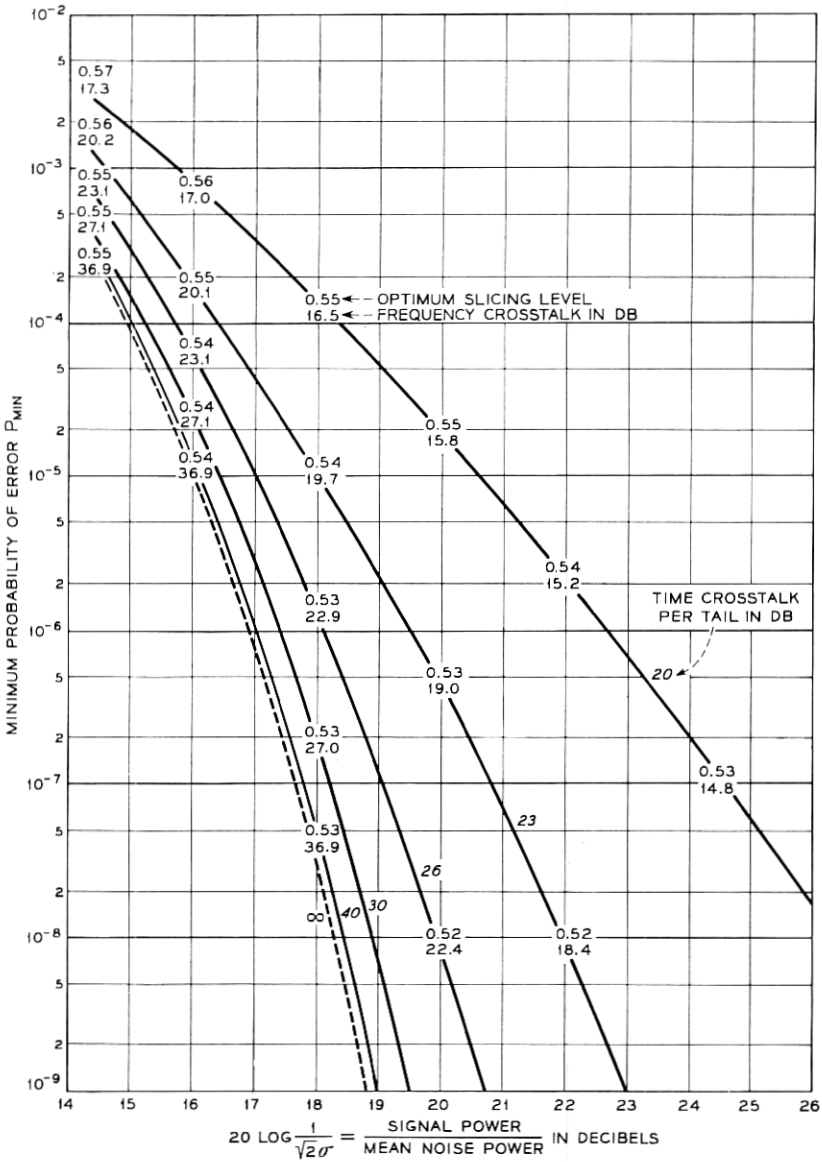

Fig. 3 — Probability of error of a message in the presence of crosstalk and noise.

For a given signal-to-noise ratio, if the normalized time crosstalk intensity per tail, ρ_T, is small compared to the normalized mean noise power $2\sigma^2$, two time-crosstalking tails introduce by themselves as many errors as does one frequency crosstalk 3 db above the level of each tail. But if $\rho_T \gg 2\sigma^2$ the time-crosstalking tails introduce as many errors as does one frequency crosstalk 6 db above the level of each tail.

For each set of values σ, ρ_T, and ρ_F that satisfies (13) we calculate from (11) the optimum slicing level ρ_0 that minimizes the probability of error, and $P_{\min}$, the value of that minimum. Fig. 3 contains this information. The probability of error, $P_{\min}$, is plotted as a function of signal-to-noise level for different values, ρ_T, of time crosstalk per tail. Each set of pairs of numbers on these curves indicates the local optimum slicing level ρ_0 and the frequency crosstalk ρ_F.

The dashed line (no crosstalk) almost coincides with that derived by Bennett.[3] The small difference stems from the fact that Bennett calculates the probability of error of the message for equal contributions of errors from the "on" and "off" pulse condition, while we calculate the minimum probability of error of the message.

IV. OPTIMUM DESIGN REGION

Suppose that we want to design a system with a given probability of error. Is there only one combination of values of crosstalk and signal-to-noise capable of satisfying the demanded probability of error? The answer is no. In Fig. 7 the given probability of error will be an ordinate obtainable with an infinite number of combinations of signal-to-noise level and crosstalk. We will develop two criteria for making a reasonable choice, and for that purpose we need some intermediate steps.

As a first step we redraw the part of Fig. 3 for low probability of error in Fig. 4, using time crosstalk per tail as the abscissa, signal-to-noise as the ordinate, and probability of error as parameter. The frequency crosstalk and optimum slicing level change slightly from point to point, but their exact values have not been written down.

As a second step we derive Fig. 5 from Figs. 6 and 7, which, together with Fig. 8, a sheet of definition of symbols, have been taken from the companion paper.[4] We shall see later how the derivation takes place, but first let us get acquainted with Figs. 6 and 7. In both these figures, the ordinates are proportional to time spacing between successive pulses, τ, times frequency spacing between adjacent channels, $|f_1 - f_2|$. The smaller this product the better, because time and frequency occupancies are proportional to the product. The different coefficients of

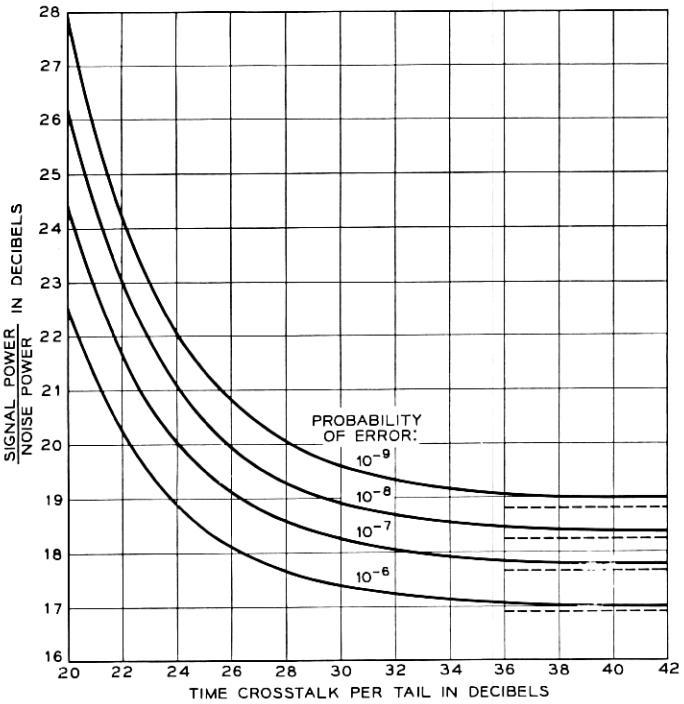

Fig. 4 — Reproduction of a section of Fig. 3, using new coordinates.

proportionality in the figures have to do with the input pulse width $2T$ and sampling time $2T_r$. The abscissas measure the ratio between bandwidth of the sending filter, $2F_1$, and the bandwidth of the receiving filter, $2F_2$. Eack figure contains three sets of curves, each corresponding to different time crosstalk per tail and different frequency crosstalk. Finally, the curves in each set correspond to different combinations of transfer characteristics of the transmitting and receiving filters.

The upper and lower dashed lines in Fig. 5 are applicable to systems with sending and receiving filters, each approximately maximally flat (three cavities); they have been derived from the dotted lines in Figs. 6 and 7, respectively. The upper and lower solid lines in Fig. 5 are applicable to systems with Gaussian sending filter and receiving filter approximately maximally flat (three cavities); they have been derived from the full lines in Figs. 6 and 7, respectively. The ordinates in Fig. 5 are the ordinates of the minimums of Figs. 6 and 7, and the abscissas

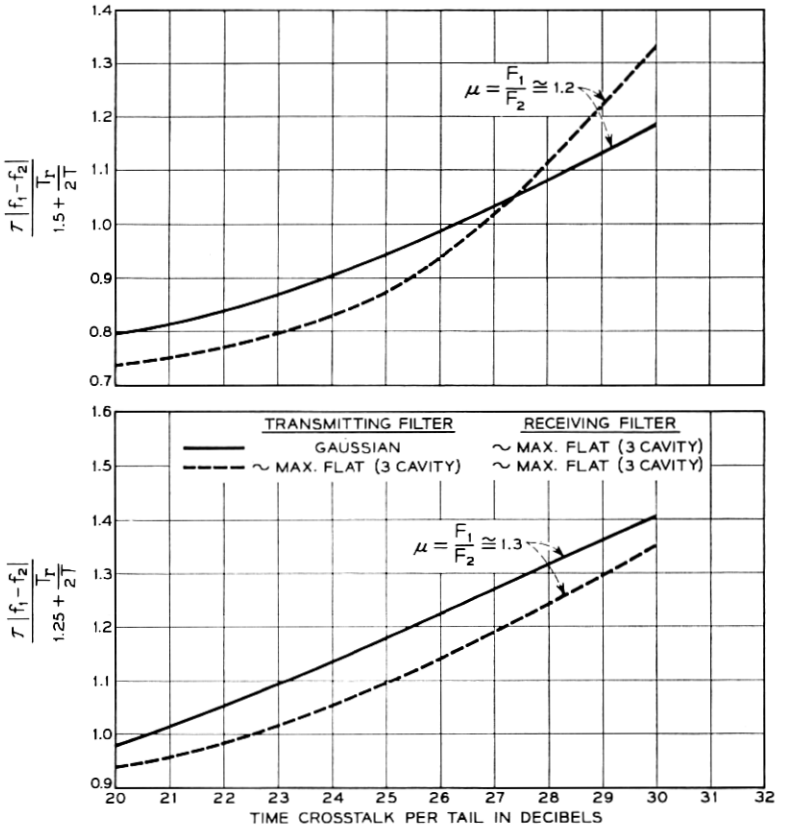

Fig. 5 — Minimum $\tau|f_1 - f_2|$.

in Fig. 5 are the different time crosstalks per tail corresponding to each set of curves in Figs. 6 and 7.

It is important to bear in mind that the ordinates of Fig. 5 are proportional to the minimum time spacing, τ, times channel frequency spacing, $|f_1 - f_2|$, which corresponds to maximum rate of information transmission.

As a third step we compare Fig. 4 with Fig. 5. For the same value of the abscissa both figures have ordinates that measure properties of the system we want to be as small as possible, but, since the slopes in the two figures are of different sign, a system operating at high time crosstalk per tail (small abscissa) will have (Fig. 5) a desirable low value $\tau|f_1 - f_2|$ but a large and unwanted signal-to-noise level. Conversely, a

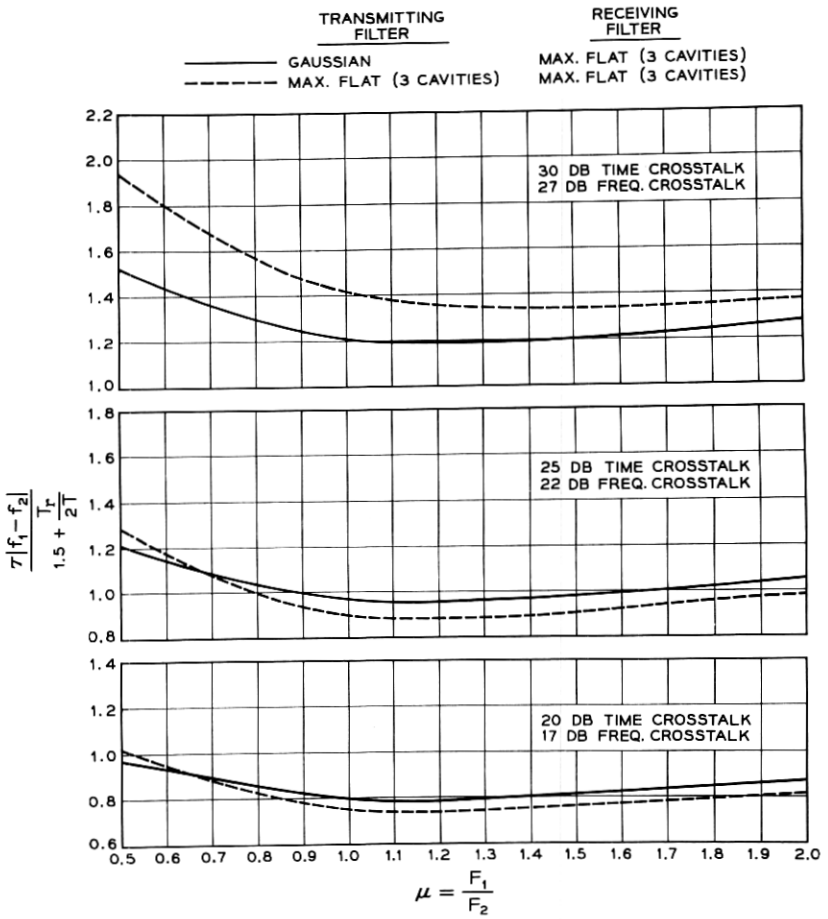

Fig. 6 — $\tau \mid f_1 - f_2 \mid$ curves for $\tau/2T = 1.5 + T_r/2T$.

system operating at low time crosstalk per tail will have an undesirably large $\tau|f_1 - f_2|$ and a wanted low signal-to-noise level. This suggests the existence of an intermediate optimum, and the question now is what function we want to minimize.

The answer is elusive, because what we really want is to minimize the price of a system that handles a certain rate of information with a given probability of error. That cost must be a function of time spacing, channel spacing, signal-to-noise ratio, and perhaps other variables. We don't know that function — at least not now — and because of lack of better knowledge we propose the minimization of two simple functions in which the signal-to-noise ratio is weighted differently:

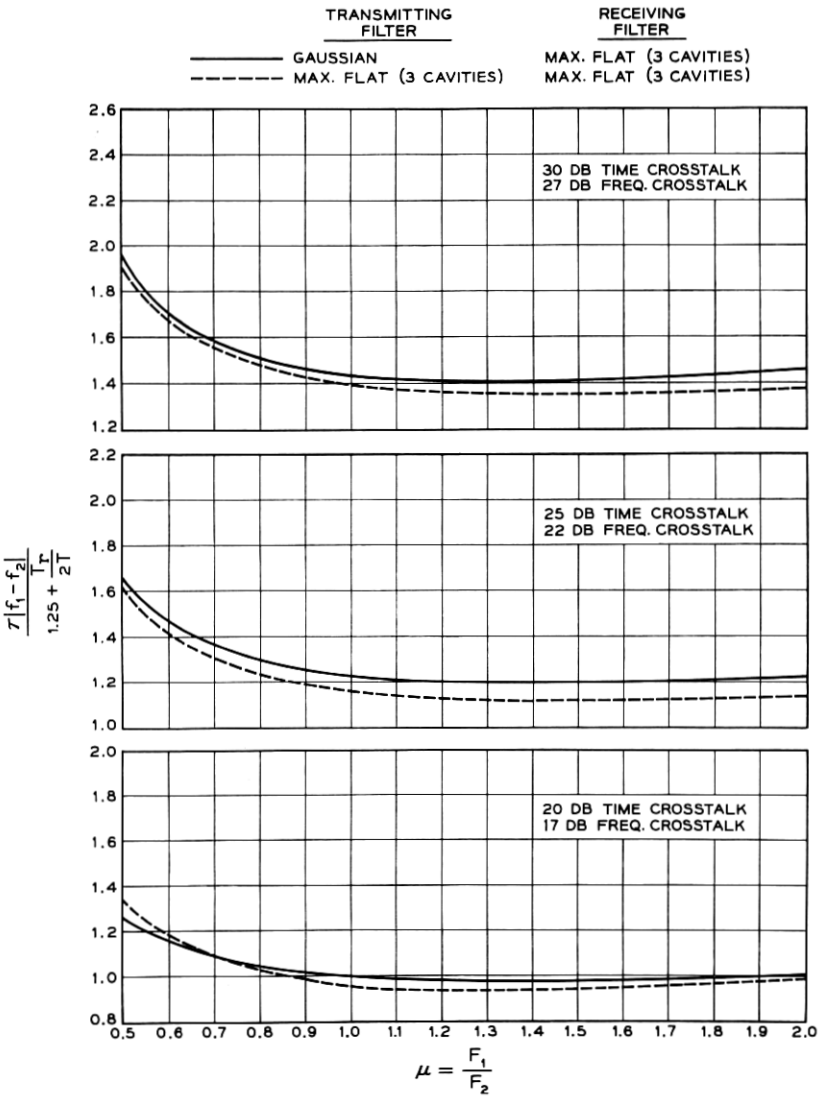

Fig. 7 — $\tau\,|f_1 - f_2|$ curves for $\tau/2T = 1.25 + T_r/2T$.

$$G_1 \propto \tau|f_1 - f_2|20 \log \frac{1}{\sqrt{2}\sigma}$$

and

$$G_2 \propto \tau|f_1 - f_2| \frac{1}{\sqrt{2}\sigma},$$

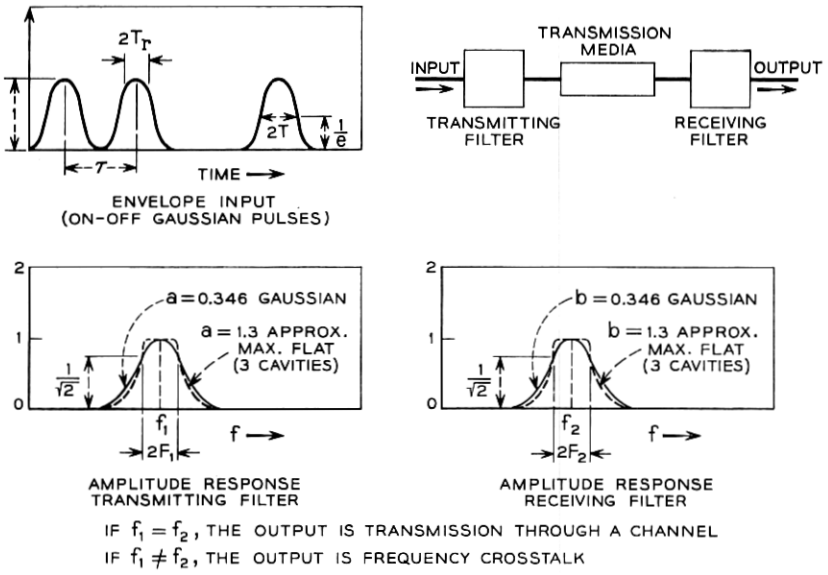

Fig. 8 — Definitions of symbols.

where 20 log $(1/\sqrt{2}\sigma)$ is the signal-to-noise in db and $1/\sqrt{2}\sigma$ is the ratio of rms signal and rms noise.

The different weighting functions were selected in order to introduce some idea about the influence of distance between successive repeaters. Since the amplitude of the received signal decays exponentially with the distance between terminals, for fixed transmitter and receiver G_1 decreases linearly with distance and G_2 decreases exponentially with distance.

Functions G_1 and G_2, obtained by multiplying the ordinates of each curve in Fig. 5 by the properly weighted ordinates of Fig. 4, have been plotted in Figs. 9, 10, 11, and 12. Each figure contains two sets of curves, and in each set the three curves exhibit minimums individualized by the coordinates probability of error and time crosstalk per tail. Those coordinates identify three points of an optimization curve that could be plotted in Fig. 3. For clarity, part of Fig. 3 has been reproduced in Fig. 13, omitting the detailed information on frequency crosstalk and optimum slicing level. In Fig. 13 we have plotted the lines joining each set of three points rather than the points themselves. Since there are eight sets of curves in Figs. 9 through 12, we get eight lines of optimum design in Fig. 13. Four of them correspond to the minimization of G_1 (signal-

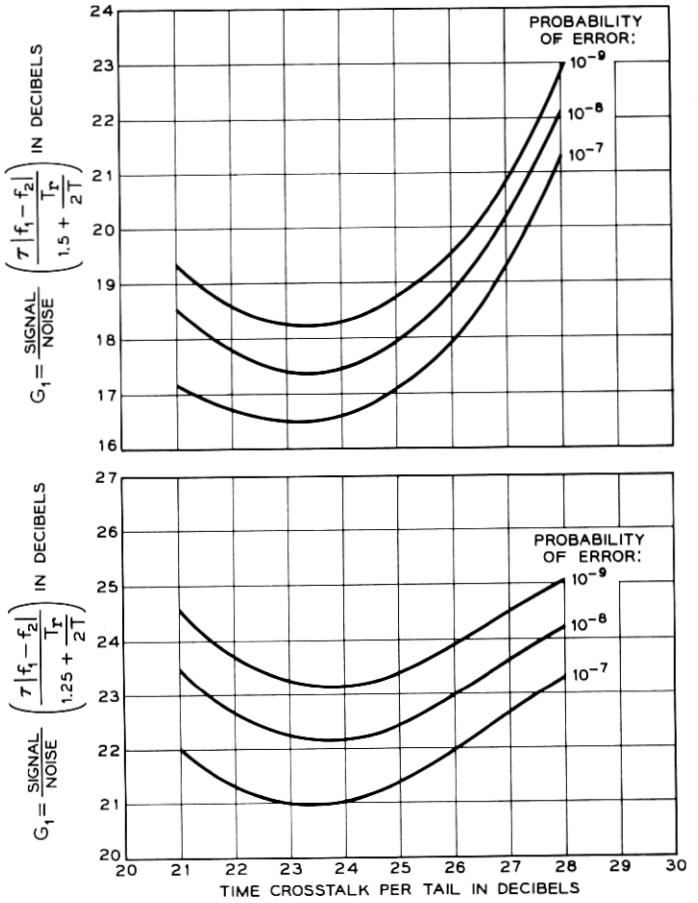

Fig. 9 — Minimization of G_1 , transmitting and receiving filters approximately maximally flat (three cavities).

to-noise in db) and are clustered close to the line defined by the parameter time crosstalk per tail 24 db; the other four lines of optimum design correspond to the minimization of G_2 (rms signal to rms noise) and are close to the line defined by the parameter time crosstalk per tail 26 db. In each cluster, the two solid lines are optimization curves for two systems, both with maximally flat (three cavities) transmitting and receiving filters but with different input pulse width $2T$ and sampling time $2T_r$; the two dashed lines are optimization curves for two systems both with Gaussian transmitting filters and maximally flat (three

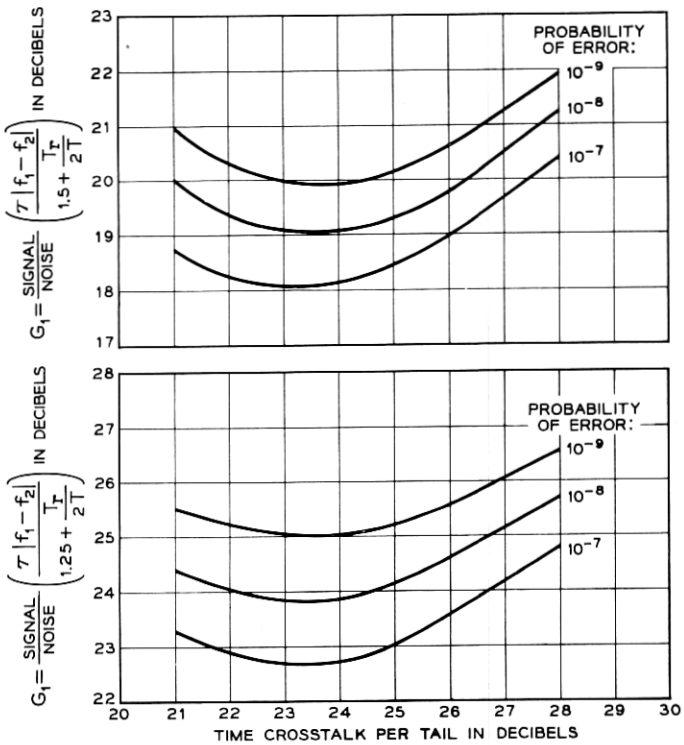

Fig. 10 — Minimization of G_1, transmitting filter Gaussian, receiving filter approximately maximally flat (three cavities).

cavities) receiving filters, but with different input pulse width $2T$ and sampling time $2T_r$.

In spite of the different dependence of signal-to-noise in G_1 and G_2, the different shapes of transmitting and receiving transfer characteristics, and the different input pulse widths and sampling times, all curves of optimum design are rather close to each other, and they are essentially located in the region where rms noise and rms crosstalk are comparable.

The optimum design lines are in general slightly steeper than the constant time crosstalk per tail lines, and, in particular, the two extremes of each of these eight design lines correspond to a change of 100 in the probability of error, around 1.5 db in signal-to-noise and only a few tenths of a db in time crosstalk per tail. This means that, once an optimum system has been built, the probability of error can be changed substantially by modifying only the signal-to-noise ratio (which is easy to do) and, in spite of this change, the system will remain close to the optimum design.

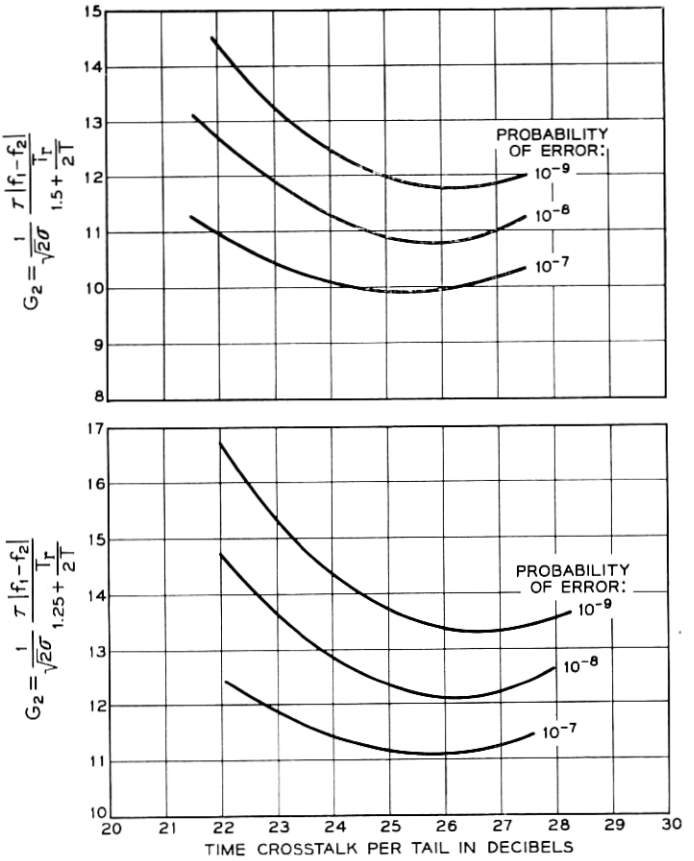

Fig. 11 — Minimization of G_2, transmitting filter Gaussian, receiving filter approximately maximally flat (three cavities).

V. CONCLUSIONS

The probability of error in the envelope detection of an RF signal embedded in Gaussian noise, time crosstalk from two neighboring pulses, and frequency crosstalk from an adjacent channel has been calculated and plotted in Fig. 3.

Also, two kinds of optimum operating conditions have been postulated which yield the results shown in Fig. 13. These conditions allow one to design a system in such a way that some minimization of time spacing between successive pulses, frequency spacing between adjacent channels, and signal-to-noise ratio is achieved.

An example of design is this: Suppose we want an optimally designed

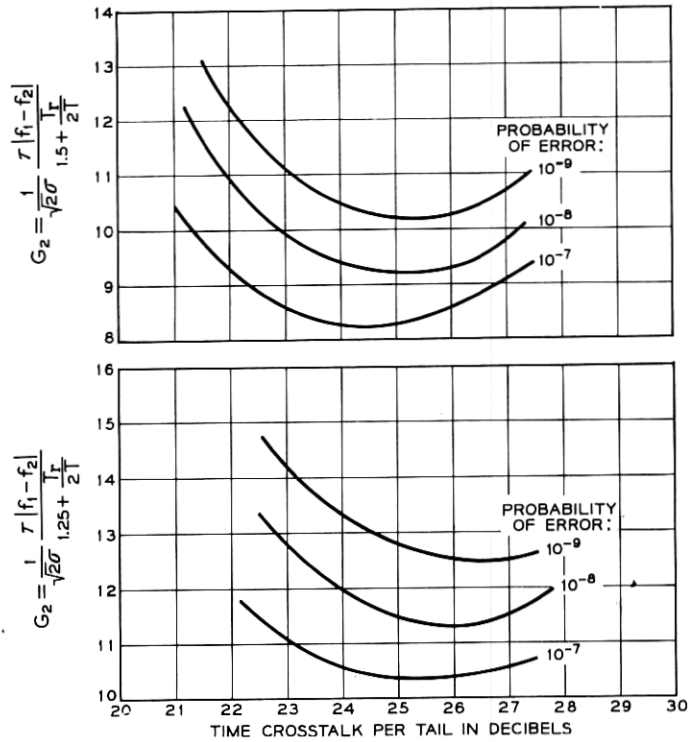

Fig. 12 — Minimization of G_2, transmitting and receiving filters approximately maximally flat (three cavities).

system that has a probability of error of 10^{-8}. We don't know which of the two criteria of optimization developed in this paper is closer to reality, and, because of that lack of knowledge, we adopt the middle of the road for the example. In Fig. 13, the ordinate 10^{-8} and the middle of the optimum design region establish that the system should have a signal-to-noise level of about 20.6 db and a time crosstalk per tail of 25 db. This last datum is enough to enter in the companion paper[4] and to complete the design of the system.

VI. ACKNOWLEDGMENT

I am indebted to Mrs. C. L. Beattie for carrying out the calculations necessary for Fig. 3.

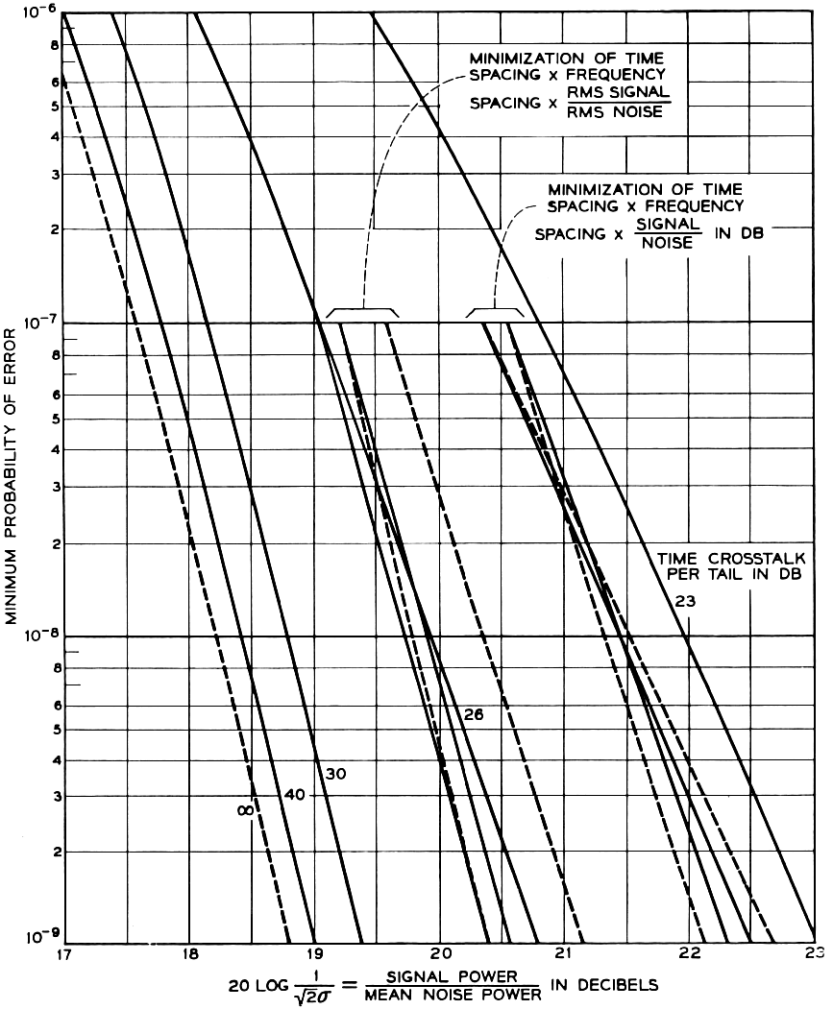

Fig. 13 — Optimum design region: solid curves — transmitting and receiving filters approximately maximally flat; dashed curves — transmitting filter Gaussian, receiving filter approximately maximally flat.

APPENDIX A

Crosstalk Between Adjacent Frequency Channels

We want to determine the frequency crosstalk between adjacent channels in order to find what arrangement of filters is the most favorable.

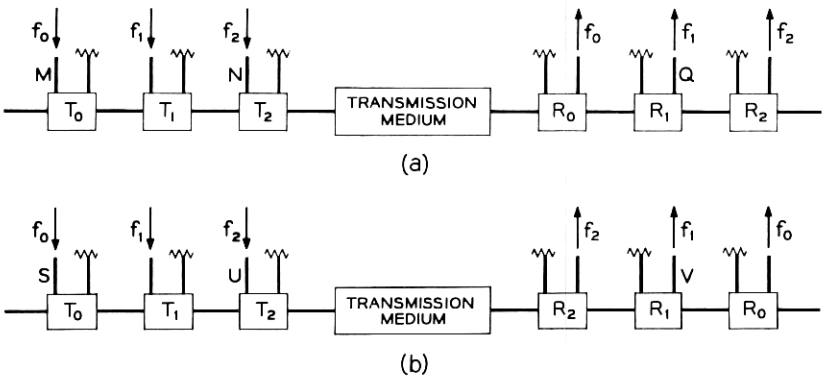

Fig. 14 — Arrangements of transmitting and receiving filters in a system.

The systems we shall deal with, shown in Figs. 14(a) and 14(b), differ in the order in which the bands are dropped. Each system consists of many transmitting and receiving filters, of which only three transmitting filters — T_0, T_1, and T_2 — and three receiving filters — R_0, R_1, and R_2 — are drawn, because we assume that the crosstalk in a receiver (R_1), comes essentially from the immediately neighboring channels.

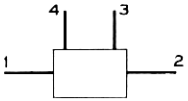

Fig. 15 — Transmitting or receiving filter.

For simplicity, we assume that, except for the frequency at which they are tuned, all the filters are similar to that shown in Fig. 15. They are constant-resistance, symmetrical, and reciprocal, and the transfer functions between terminals are given by the scattering matrix

$$S = \begin{vmatrix} S_{11} & S_{12} & S_{13} & S_{14} \\ S_{21} & S_{22} & S_{23} & S_{24} \\ S_{31} & S_{32} & S_{33} & S_{34} \\ S_{41} & S_{42} & S_{43} & S_{44} \end{vmatrix}$$

$$= \begin{vmatrix} 0 & i\sqrt{1-Y^2} & Y & 0 \\ i\sqrt{1-Y^2} & 0 & 0 & Y \\ Y & 0 & 0 & i\sqrt{1-Y^2} \\ 0 & Y & i\sqrt{1-Y^2} & 0 \end{vmatrix}. \tag{16}$$

Now we can calculate the maximum intensity of the crosstalk C_{MQ} between M and Q in Fig. 14(a) due to a pulse entering at M.

Assuming for simplicity that the system is phase equalized and that the input pulse has a $(\sin x)/x$ shape (rectangular spectrum), the maximum intensity of the crosstalk is given by

$$C_{MQ} = K \int_0^\infty G_0 Y_0 \sqrt{1 - Y_1^2} \sqrt{1 - Y_2^2} \sqrt{1 - Y_0^2}\, Y_1\, df, \quad (17)$$

where K is a constant of proportionality, G_0 is the rectangular spectrum of the input pulse centered at f_0, and $Y_0\sqrt{1 - Y_1^2}\sqrt{1 - Y_0}\, Y_1$ derived from (16), and Fig. 14(a) is the transfer function between M and Q. The subindices 0 and 1 refer to the center frequencies f_0 and f_1 of each scattering coefficient.

Following arguments similar to the preceding one, the maximum crosstalk intensities between N and Q in Fig. 14(a) and between S and V and between U and V in Fig. 14(b), are

$$C_{NQ} = K \int_0^\infty G_2 Y_2 \sqrt{1 - Y_0^2}\, Y_1\, df, \quad (18)$$

$$C_{SV} = K \int_0^\infty G_0 Y_0 \sqrt{1 - Y_1^2}\,(1 - Y_2^2) Y_1\, df, \quad (19)$$

$$C_{UV} = K \int_0^\infty G_2 Y_2 \sqrt{1 - Y_2^2}\, Y_1\, df. \quad (20)$$

The factors involved in each integrand of (17) through (20) have been plotted in Figs. 16(a), (b), (c), and (d). The integrands of (17) through (20) are obtained by multiplying the curves in Fig. 16(a) through Fig. 16(d) respectively. The results which happen to be the output spectra are plotted in Fig. 17(a) through Fig. 17(d).

The integration of these curves with respect to frequency, that is, the areas between the curves and the frequency axes, are, because of (17) through (20), proportional to the maximum intensities of the crosstalks.

Comparing these areas we deduce

$$C_{MQ} = C_{UV}, \quad (21)$$

$$C_{NQ} = C_{SV}, \quad (22)$$

$$C_{MQ} \ll C_{NQ}, \quad (23)$$

$$C_{UV} \ll C_{SV}. \quad (24)$$

The first two equations show that the total crosstalk in the system of

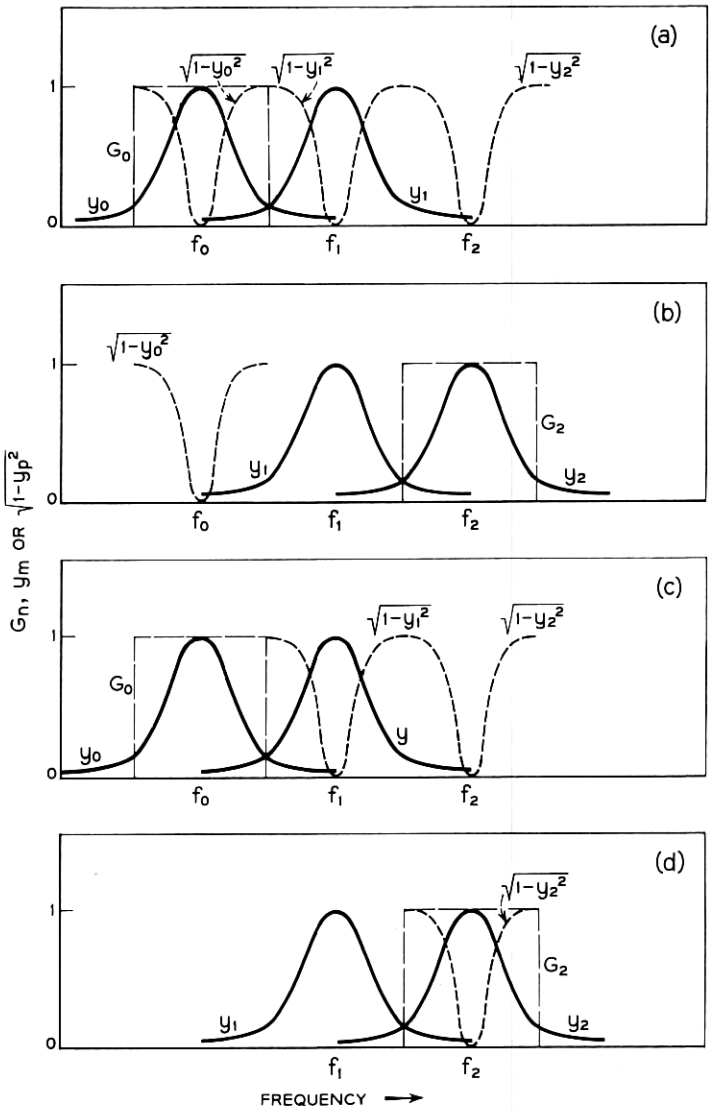

Fig. 16 — Factors involved in integrands of (17) through (20); G_n = input signal spectra; Y_m , $\sqrt{1 - Y_p^2}$ = scattering coefficients.

Fig. 14(a) is the same as the total crosstalk in the system of Fig. 14(b). Furthermore, from (23) and (24) we deduce that the total crosstalk in either system comes from the superposition of two signals, of which one is negligible compared to the other.

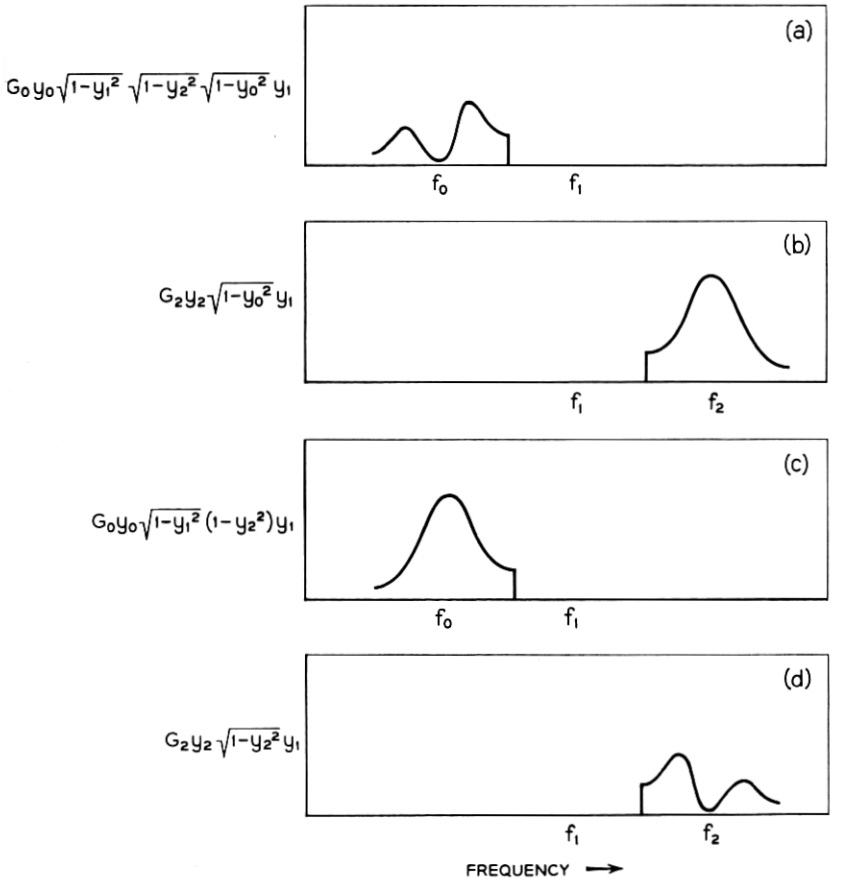

Fig. 17 — Spectra of crosstalk signals.

APPENDIX B

Bivariate Density Distribution

An on-off pulse embedded in unwanted crosstalk and noise is represented vectorially by

$$S = A + \rho_T e^{i\theta_1} + \rho_T e^{i\theta_2} + \rho_F e^{i\theta_3} + \text{Gaussian noise.} \qquad (25)$$

The amplitude A of the RF pulse is unity if the pulse is on, and zero if the pulse is off; the phase of this vector is selected zero, as reference. Time crosstalk is represented by two vectors of the same modulus ρ_T and arbitrary phases θ_1 and θ_2. Frequency crosstalk is represented by a

vector of modulus ρ_F and arbitrary phase θ_3. Each one of these three vectors, since it originated from binary pulses, has equal probability of being present or not. The phases θ_1, θ_2, and θ_3 have a constant probability of acquiring any value between zero and 2π.

We want to calculate the density distribution of S, and we know the density distribution of each one of its five uncorrelated terms:

$$p_1(x,y) = \delta(x - A)\delta(y), \tag{26}$$

$$p_2(x,y) = p_3(x,y) = \frac{\delta(\sqrt{x^2 + y^2})}{4\pi\sqrt{x^2 + y^2}} + \frac{\delta(\sqrt{x^2 + y^2} - \rho_T)}{4\pi\,\rho_T}, \tag{27}$$

$$p_4(x,y) = \frac{\delta(\sqrt{x^2 + y^2})}{4\pi\sqrt{x^2 + y^2}} + \frac{\delta(\sqrt{x^2 + y^2} - \rho_F)}{4\pi\,\rho_F}, \tag{28}$$

$$p_5(x,y) = \frac{1}{2\pi\sigma^2} e^{-(x^2+y^2)/2\sigma^2}, \tag{29}$$

where $\delta(z)$ is the Dirac delta function and σ^2 is the variance, which in this particular problem measures the mean noise power.

It is known that the distribution $p(x,y)$ of the sum S of independent terms is equal to the inverse transform of the product of the double Fourier transform of the density distribution of each term of the sum.[3]

The double Fourier transform of a distribution $p_n(x,y)$ is, by definition

$$C_n = \iint_{-\infty}^{\infty} e^{i(\xi x+\eta y)} p_n(x,y)\, dx\, dy. \tag{30}$$

Replacing $p_n(x,y)$ by (26) through (29) and integrating,

$$C_1 = e^{i\xi A}, \tag{31}$$

$$C_2 = C_3 = \tfrac{1}{2}[1 + J_0(\rho_T\sqrt{\xi^2 + \eta^2})], \tag{32}$$

$$C_4 = \tfrac{1}{2}[1 + J_0(\rho_F\sqrt{\xi^2 + \eta^2})], \tag{33}$$

$$C_5 = e^{-(\sigma^2/2)(\xi^2+\eta^2)}, \tag{34}$$

where J_0 is the Bessel function of first order and kind.

The inverse transform of the product of these functions is the distribution $p(x,y)$ of the signal S we were looking for:

$$p(x,y) = \frac{1}{32\pi^2} \iint_{-\infty}^{\infty} e^{-i[\xi(x-A)+\eta y]-(\sigma^2/2)(\xi^2+\eta^2)}[1 + J_0(\rho_T\sqrt{\xi^2 + \eta^2})]^2 \cdot[1 + J_0(\rho_F\sqrt{\xi^2 + \eta^2})]\, d\xi\, d\eta. \tag{35}$$

The distribution $p(x,y)$ is the summation of several double integrals to be evaluated. The most general of them is

$$W = \iint_{-\infty}^{\infty} e^{-i[\xi(x-A)+\eta y]-(\sigma^2/2)(\xi^2+\eta^2)} J_0(\rho_1\sqrt{\xi^2+\eta^2}) \cdot J_0(\rho_2\sqrt{\xi^2+\eta^2}) J_0(\rho_3\sqrt{\xi^2+\eta^2})\, d\xi\, d\eta. \tag{36}$$

Replacing each Bessel function by an integral expression,[5]

$$W = \frac{1}{(2\pi)^3} \iiint_0^{2\pi} d\alpha\, d\beta\, d\gamma \iint_{-\infty}^{\infty} e^{-i\xi[(x-A)-\rho_1\cos\alpha-\rho_2\cos\beta-\rho_3\cos\gamma]} \cdot e^{-i\eta(y-\rho_1\sin\alpha-\rho_2\sin\beta-\rho_3\sin\gamma)-(\sigma^2/2)(\xi^2+\eta^2)}\, d\xi\, d\eta. \tag{37}$$

The two integrations from $-\infty$ to ∞ are known Fourier transforms, and (37) becomes

$$W = \frac{1}{(2\pi\sigma)^2} \cdot \iiint_0^{2\pi} e^{[(x-A-\rho_1\cos\alpha-\rho_2\cos\beta-\rho_3\cos\gamma)^2-(y-\rho_1\sin\alpha-\rho_2\sin\beta-\rho_3\sin\gamma)^2]/2\sigma^2} d\alpha\, d\beta\, d\gamma. \tag{38}$$

By changing variables,

$$\begin{aligned} x - A &= r\cos\varphi, \\ y &= r\sin\varphi \end{aligned} \tag{39}$$

the exponent can be rearranged:

$$W = \frac{e^{-(r^2+\rho_1^2+\rho_2^2+\rho_3^2)/2\sigma^2}}{(2\pi\sigma)^2} \cdot \iiint_0^{2\pi} e^{[r\rho_1\cos(\alpha-\varphi)+r\rho_2\cos(\beta-\varphi)+r\rho_3\cos(\gamma-\varphi) -\rho_1\rho_2\cos(\alpha-\beta)-\rho_1\rho_3\cos(\alpha-\gamma)-\rho_2\rho_3\cos(\beta-\gamma)]/\sigma^2} d\alpha\, d\beta\, d\gamma. \tag{40}$$

We start integrating with respect to α. The integral to be solved is essentially

$$W_\alpha = \int_0^{2\pi} e^{\rho_1[r\cos(\alpha-\varphi)-\rho_2\cos(\alpha-\beta)-\rho_3\cos(\alpha-\gamma)]/\sigma^2} d\alpha. \tag{41}$$

The exact result is[3]

$$W_\alpha = 2\pi I_0\left(\frac{\rho_1}{\sigma^2}\sqrt{\begin{matrix}[r-\rho_2\cos(\varphi-\beta)-\rho_3\cos(\varphi-\gamma)]^2 \\ +[\rho_2\sin(\varphi-\beta)+\rho_3\sin(\varphi-\gamma)]^2\end{matrix}}\right), \quad (42)$$

but if we carry this expression to (40) the integration with respect to β and γ becomes extremely complicated.

A substantial simplification can be obtained if we consider first that we are interested only in the tails of the distributions, and consequently

$$r \gg \begin{cases}\rho_1 \\ \rho_2 \\ \rho_3\end{cases}. \quad (43)$$

Second, for

$$\left.\begin{matrix}\frac{r\rho_1}{\sigma^2} \\ \frac{r\rho_2}{\sigma^2} \\ \frac{r\rho_3}{\sigma^2}\end{matrix}\right\} \gg 1, \quad (44)$$

which is the only nontrivial case, the main contribution to the triple integral (40) comes from values of the integrating variables

$$\left.\begin{matrix}\alpha \\ \beta \\ \gamma\end{matrix}\right\} \cong \varphi. \quad (45)$$

Because of (43) and (45), expression (41) can be reduced to

$$W_\alpha \cong e^{-\rho_1[(\rho_2+\rho_3)/\sigma^2]}\int_0^{2\pi} e^{(\rho_1 r/\sigma^2)\cos(\alpha-\varphi)}\,d\varphi \quad (46)$$

and, after performing the integration,

$$W_\alpha \cong 2\pi e^{-\rho_1[(\rho_2+\rho_3)/\sigma^2]}\, I_0\left(\frac{\rho_1 r}{\sigma^2}\right). \quad (47)$$

The reader may also derive this result from (42), (43), and (45). Substituting this result of the integration on α, in (40),

$$W = \frac{e^{(r^2+\rho_1{}^2+\rho_2{}^2+\rho_3{}^2+2\rho_1\rho_2+2\rho_1\rho_3)/2\sigma^2}}{2\pi\sigma^2} I_0\left(\frac{\rho_1 r}{\sigma^2}\right) \cdot \int_0^{2\pi}\int e^{[r\rho_2 \cos(\beta-\varphi)+r\rho_3 \cos(\gamma-\varphi)-\rho_2\rho_3 \cos(\beta-\gamma)]/\sigma^2} d\beta\, d\gamma. \quad (48)$$

Now we perform the integration on β. The integral to be solved is essentially

$$W_\beta = \int_0^{2\pi} e^{(\rho_2/\sigma^2)[r\cos(\beta-\varphi)-\rho_3\cos(\beta-\gamma)]}\, d\beta. \quad (49)$$

Following the same reasoning used to integrate W_α, in (41), the approximate result is

$$W_\beta \cong 2\pi e^{-\rho_2\rho_3/\sigma^2} I_0\left(\frac{\rho_2 r}{\sigma^2}\right). \quad (50)$$

After substituting in (48) and performing the integration on γ, W is

$$W = \frac{2\pi}{\sigma^2} e^{-[r^2+(\rho_1+\rho_2+\rho_3)^2]/2\sigma^2} I_0\left(\frac{\rho_1 r}{\sigma^2}\right) I_0\left(\frac{\rho_2 r}{\sigma^2}\right) I_0\left(\frac{\rho_3 r}{\sigma^2}\right). \quad (51)$$

Substituting this generic result in (35), the density distribution of the signal S is obtained:

$$p(x,y) = \frac{e^{-r^2/2\sigma^2}}{16\pi\sigma^2}\left[1 + 2e^{-\rho_T{}^2/2\sigma^2} I_0\left(\frac{\rho_T r}{\sigma^2}\right) + e^{-2\rho_T{}^2/\sigma^2} I_0{}^2\left(\frac{\rho_T r}{\sigma^2}\right) + e^{-\rho_F{}^2/2\sigma^2} I_0\left(\frac{\rho_F r}{\sigma^2}\right) + 2e^{-(\rho_T+\rho_F)^2/2\sigma^2} I_0\left(\frac{\rho_T r}{\sigma^2}\right) I_0\left(\frac{\rho_F r}{\sigma^2}\right) + e^{-(2\rho_T+\rho_F)^2/2\sigma^2} I_0{}^2\left(\frac{\rho_T r}{\sigma^2}\right) I_0\left(\frac{\rho_F r}{\sigma^2}\right)\right]. \quad (52)$$

APPENDIX C

Evaluation of Probabilities of Error

Case 1: "Pulse On"

We want to evaluate the integral

$$P_1 = \int_{a_1} p_1(x,y)\, dx\, dy, \quad (53)$$

where a_1 is a circle of radius $\rho_0 \cong \frac{1}{2}$ with center at the origin of coordinates, and $p_1(x,y)$ is obtained from (52) by making

$$A = 1 \quad (54)$$

in the expression

$$r = \sqrt{(x - A)^2 + y^2}. \tag{55}$$

Adopting the following change of variables:

$$\begin{aligned} x &= \rho \cos \psi, \\ y &= \rho \sin \psi, \end{aligned} \tag{56}$$

P_1 becomes

$$P_1 = \int_{-\pi}^{\pi} \int_0^{\rho_0} p_1(\rho \cos \psi, \rho \sin \psi)\, d\rho\, d\psi. \tag{57}$$

The most general term of the integration is proportional to

$$U_1 = \int_{-\pi}^{\pi} \int_0^{\rho_0} e^{-r^2/2\sigma^2} I_0\left(\frac{\rho_1 r}{\sigma^2}\right) I_0\left(\frac{\rho_2 r}{\sigma^2}\right) I_0\left(\frac{\rho_3 r}{\sigma^2}\right) \rho\, d\psi\, d\rho, \tag{58}$$

where

$$r = \sqrt{1 + \rho^2 - 2\rho \cos \psi}. \tag{59}$$

We simplify the integrand. Notice first that, since

$$\rho_0 \cong \tfrac{1}{2}, \tag{60}$$

we deduce, from (59),

$$r > \tfrac{1}{2}$$

independently of ψ; second, the range of interest for σ is

$$\sigma \ll \rho_0 . \tag{61}$$

Therefore, the exponent in (58) is

$$\frac{r^2}{2\sigma^2} \gg 1. \tag{62}$$

Because of this inequality and because, for a small variation of r, the exponential in (58) varies much faster than the modified Bessel functions, most of the contribution to the integral comes from values of the variable close to those that minimize r,

$$\begin{aligned} \psi &= 0, \\ \rho &= \rho_0 , \end{aligned}$$

and (58) becomes

$$U_1 \cong I_0\left(\rho_1 \frac{1 - \rho_0}{\sigma^2}\right) I_0\left(\rho_2 \frac{1 - \rho_0}{\sigma^2}\right) I_0\left(\rho_3 \frac{1 - \rho_0}{\sigma^2}\right) D, \tag{63}$$

where

$$D = \int_{-\pi}^{\pi} \int_0^{\rho_0} e^{-(1+\rho^2-2\rho \cos \psi)/2\sigma^2} \rho\, d\psi\, d\rho. \tag{64}$$

Integrating with respect to ψ,

$$D = 2\pi \int_0^{\rho_0} e^{-(1+\rho^2)/2\sigma^2} I_0\left(\frac{\rho}{\sigma^2}\right) \rho \, d\rho. \tag{65}$$

Since the exponential varies much faster than the rest of the integrand, most of the contribution to the integral comes from $\rho \cong \rho_0$, and, because of (60) and (61), $I_0(\rho/\sigma^2)$ can be replaced by its asymptotic expansion. Consequently,

$$D \cong \sqrt{2\pi\rho_0}\, \sigma \int_0^{\rho_0} e^{-(1-\rho)^2/2\sigma^2} \, d\rho. \tag{66}$$

Integrating,

$$D = \sqrt{2\pi\rho_0}\, \frac{\sigma^3}{1 - \rho_0} e^{-(1-\rho_0)^2/2\sigma^2}; \tag{67}$$

for compactness, this can be rewritten

$$D \cong \sigma^2 K_0\left[\frac{(1 - \rho_0)^2}{2\sigma^2}\right], \tag{68}$$

where K_0 is the modified Bessel function of the second kind.

Substituting (68) in (63), the general term of the integration (57) is

$$U_1 = \sigma^2 K_0\left[\frac{(1 - \rho_0)^2}{2\sigma^2}\right] I_0\left(\rho_1 \frac{1 - \rho_0}{\sigma^2}\right) I_0\left(\rho_2 \frac{1 - \rho_0}{\sigma^2}\right) I_0\left(\rho_3 \frac{1 - \rho_0}{\sigma^2}\right) \tag{69}$$

and the probability of error for the "pulse on" condition is

$$\begin{aligned} P_1 = \frac{K_0\left[\frac{(1 - \rho_0)^2}{2\sigma^2}\right]}{16\pi} \Bigg[& 1 + 2e^{-\rho_T^2/2\sigma^2} I_0\left(\rho_T \frac{1 - \rho_0}{\sigma^2}\right) \\ & + e^{-2\rho_T^2/\sigma^2} I_0^2\left(\rho_T \frac{1 - \rho_0}{\sigma^2}\right) + e^{-\rho_F^2/2\sigma^2} I_0\left(\rho_F \frac{1 - \rho_0}{\sigma^2}\right) \\ & + 2e^{(\rho_T+\rho_F)^2/2\sigma^2} I_0\left(\rho_T \frac{1 - \rho_0}{\sigma^2}\right) I_0\left(\rho_F \frac{1 - \rho_0}{\sigma^2}\right) \\ & + e^{-(2\rho_T+\rho_F)^2/2\sigma^2} I_0^2\left(\rho_T \frac{1 - \rho_0}{\sigma^2}\right) I_0\left(\rho_F \frac{1 - \rho_0}{\sigma^2}\right) \Bigg]. \end{aligned} \tag{70}$$

Case 2: "Pulse Off"

We want to evaluate the integral

$$P_2 = \int_{a_2} p_2(x,y) \, dx \, dy, \tag{71}$$

where a_2 is the surface outside of a circle of radius ρ_0 with center at the origin of coordinates, and $p_2(x,y)$ is obtained from (52) by making

$$A = 0 \tag{72}$$

in the expression

$$r = \sqrt{(x - A)^2 + y^2}.$$

After changing the variables according to (56), the ψ dependence disappears from $p_2(x,y)$ and the probability of error (71) is

$$P_2 = 2\pi \int_{\rho_0}^{\infty} p_2(r) r \, dr. \tag{73}$$

The most general term of this integral is proportional to

$$U_2 = \int_{\rho_0}^{\infty} e^{-r^2/2\sigma^2} I_0\left(\frac{\rho_1 r}{\sigma^2}\right) I_0\left(\frac{\rho_2 r}{\sigma^2}\right) I_0\left(\frac{\rho_3 r}{\sigma^2}\right) r \, dr. \tag{74}$$

Over the range of integration,

$$\frac{r^2}{2\sigma^2} \gg 1; \tag{75}$$

also, for a small variation of r, the exponential varies much faster than the modified Bessel functions. Consequently,

$$\begin{aligned} U_2 &\cong I_0\left(\frac{\rho_1\rho_0}{\sigma^2}\right) I_0\left(\frac{\rho_2\rho_0}{\sigma^2}\right) I_0\left(\frac{\rho_3\rho_0}{\sigma^2}\right) \int_{\rho_0}^{\infty} e^{-r^2/2\sigma^2} r \, dr \\ &\cong \sigma^2 e^{-{\rho_0}^2/2\sigma^2} I_0\left(\frac{\rho_1\rho_0}{\sigma^2}\right) I_0\left(\frac{\rho_2\rho_0}{\sigma^2}\right) I_0\left(\frac{\rho_3\rho_0}{\sigma^2}\right). \end{aligned} \tag{76}$$

Substituting this result in (73), we get

$$\begin{aligned} P_2 = \frac{e^{-{\rho_0}^2/2\sigma^2}}{8} \Bigg[& 1 + 2e^{-{\rho_T}^2/2\sigma^2} I_0\left(\frac{\rho_T\rho_0}{\sigma^2}\right) + e^{-2{\rho_T}^2/\sigma^2} I_0^2\left(\frac{\rho_T\rho_0}{\sigma^2}\right) \\ & + e^{-{\rho_F}^2/2\sigma^2} I_0\left(\frac{\rho_F\rho_0}{\sigma^2}\right) + 2e^{-(\rho_T+\rho_F)^2/2\sigma^2} I_0\left(\frac{\rho_T\rho_0}{\sigma^2}\right) I_0\left(\frac{\rho_F\rho_0}{\sigma^2}\right) \\ & + e^{-(2\rho_T+\rho_F)^2/2\sigma^2} I_0^2\left(\frac{\rho_T\rho_0}{\sigma^2}\right) I_0\left(\frac{\rho_F\rho_0}{\sigma^2}\right) \Bigg]. \end{aligned} \tag{77}$$

REFERENCES

1. Miller, S. E., Waveguide as a Communication Medium, B.S.T.J., **33**, 1954, p. 1209.
2. Sunde, E. D., Ideal Binary Pulse Transmission by AM and FM, B.S.T.J., **37**, 1959, p. 1357.
3. Bennett, W. R., Methods of Solving Noise Problems, Proc. I.R.E., **44**, 1956, p. 609.
4. Marcatili, E. A., Time and Frequency Crosstalk in Pulse-Modulated Systems, this issue, p. 951.
5. Jahnke, E., and Emde, F., *Tables of Functions*, Dover Publications, New York, 1943, p. 149.